

THE DISTANCE TO M5 FROM ITS RR LYRAE VARIABLES

J. G. COHEN AND G. A. GORDON

Palomar Observatory, California Institute of Technology

Received 1986 November 7; accepted 1986 December 17

ABSTRACT

We have applied a variation of the Baade-Wesselink method to four RR Lyrae variables in the moderately metal-poor globular cluster M5. The radial velocity curves are from observations with the 200 inch (5 m) Hale telescope, while the photometry is derived from CCD images through a Johnson *B* and a near-infrared *i* filter. The method developed for the analysis utilizes an effective wavelength for each filter and relies on the accuracy of the calibration of absolute flux for bright standard stars by Oke and Gunn, as well as on the accuracy of the absolute emitted fluxes predicted in the near-infrared by the Kurucz grid of model stellar atmospheres.

The results must be viewed as preliminary thus far due to apparent discrepancies between the photometrically and spectroscopically deduced angular diameter-phase relationships which are most apparent in the part of the cycle immediately following maximum light. This restricts the range of phase that can be used to derive the distance to the variables. The best value we obtain for the mean of the 4 RR Lyrae stars in M5 is an absorption-corrected intensity mean absolute *V* magnitude of +1.05 mag (+0.15, -0.25 mag).

Subject headings: clusters: globular — stars: RR Lyrae

I. INTRODUCTION

The distances to globular clusters are usually determined by fixing the absolute magnitude of their horizontal-branch stars at the location of the RR Lyrae variable gap. The assumed value for the absolute luminosity of RR Lyrae variables rests upon statistical parallaxes for field RR Lyrae stars and on variations of the Baade-Wesselink (Baade 1926; Wesselink 1969) method for field RR Lyrae stars. Distances to globular clusters which rely on main-sequence locations as defined by field subdwarfs such as in Sandage (1970) or Carney (1980) suffer from the serious limitation of the extremely small number of field subdwarfs which have accurate parallaxes, and of the need to include corrections to the luminosity for varying metallicities. Many of the field subdwarfs may be slightly evolved, and thus have higher somewhat luminosities than the true main sequence.

These cluster distances are then used to determine globular cluster ages, and small errors in distance propagate into substantial age uncertainties. In addition, since RR Lyrae stars have been detected in the field and clusters of the Magellanic Clouds (Graham 1984; Graham and Nemec 1984) and in M31 (Pritchett and van den Bergh 1986) from the ground, and will undoubtedly be found in additional galaxies by the Hubble Space Telescope, their absolute magnitudes directly calibrate the extragalactic distance scale. They also serve to determine the distance to the Galactic center (Oort and Plaut 1975).

In recent years, major efforts have been undertaken by several groups to improve the absolute magnitude determinations for field RR Lyrae variables. These include the reanalysis of the statistical parallax problem with improved astrometric data by two independent groups (Hawley *et al.* 1986; Barnes and Hawley 1986; Strugnell, Reid, and Murray 1986). Manduca and Bell (1981), Manduca *et al.* (1981), Carney and Latham (1984), Jones *et al.* (1987*a, b*), Burki and Meylan (1986*a, b*), Longmore *et al.* (1985), Jameson (1986), and Cacciari (1986) have explored variations of the Baade-Wesselink technique. Major surveys are now underway to accumulate observational data which will allow such determinations of

distances for statistically significant samples of field RR Lyrae stars over a range of metallicity. While several unresolved problems remain in the analysis of the field variables, substantial progress has been made.

It is clear that the efficiency of modern detectors allows the same techniques to be applied to RR Lyrae variables in globular clusters, and that is the goal of the present effort. A natural candidate is the globular cluster M5. It has low interstellar reddening, about 100 RR Lyrae variables (Hogg 1973), a recent analysis of the periods of the M5 variables by Coutts and Sawyer-Hogg (1969), is relatively nearby so that the variables are as bright as possible, and is accessible from a northern site. In § II we present the extensive observational material we have accumulated for the RR Lyrae variables in M5 during the 1985 and 1986 observing season. The technique of analysis that we have developed is described in § III. Section IV*a* begins with a description of the results of this analysis and then continues in § IV*b* with a comparison to recent results for field stars. A summary of our conclusions is given in the final section.

II. OBSERVATIONAL MATERIAL FOR THE M5 RR LYRAES

a) Radial Velocities

The RR Lyrae variables in M5 were identified from the chart in Bailey (1917). The periods for the variables were taken directly from Hogg (1973). Because the data were taken over a range of time which for two stars was less than 1 month, for one variable was less than 6 weeks, and at the worst was only 1 year, no adjustments to the periods were necessary. (We did check at various points whether small changes in the adopted periods improved the light or radial velocity curves, but never found any definite indication of that.) The zero of our phase system is taken as the first maximum in light for each variable after Julian day 2,446,536.500 (equivalent to 0 hours UT on 1986 April 16). The fundamental data for the RR Lyrae variables discussed here is given in Table 1, which includes their periods, the zero of our phase system, the maximum and

TABLE 1
LIGHT CURVE PARAMETERS FOR M5 RR LYRAE STARS

RR Lyrae Number	Period (days)	Φ_0 (Julian days)	B_{\max} (mag)	B_{\min} (mag)	i_{\max} (mag)	i_{\min} (mag)	V_{\max} (mag)	V_{\min} (mag)	$\langle V_0 \rangle$ (mag)	Intensity Mean V_0 (mag)
8.....	0.5462306	2,446,536.505	14.67	16.01	14.92	15.60	14.53	15.51	15.08	15.04
12.....	0.467716	2,446,536.967	14.40	16.05	14.90	15.71	14.40	15.50	15.09	15.03
32.....	0.45778654	2,446,536.587	14.39	15.97	14.85	15.65	14.38	15.53	15.08	15.01
59.....	0.5420257	2,446,536.791	14.59	15.85	14.79	15.35	14.43	15.32	14.92	14.88
18.....	0.464098	2,446,536.838	14.69	15.89	14.97	15.50	14.57	15.45	15.05	15.01
19.....	0.469965	2,446,536.656	14.40	16.05	14.85	15.68	14.35	15.56	15.12	15.05
28.....	0.5439272	2,446,536.666	14.72	(15.96)	14.92	(15.44)	14.55	(15.48)	15.07	15.03
31.....	0.30058294	(2,446,536.731)	15.02	15.67	15.24	15.55	14.85	15.36	15.03	15.02
79.....	0.33313838	2,446,536.814	15.01	(15.55)	15.03	(15.27)	14.77	(15.15)	14.88	14.87

minimum magnitudes in B , i , and V , and the absorption corrected mean and intensity mean V magnitude (see § IIb).

The RR Lyrae stars chosen for analysis in M5 included only stars for which Coutts and Sawyer-Hogg (1969) found no evidence for the presence of the Blashko effect. Their extensive photographic archives made it possible for them to identify the presence of even modest cycle-to-cycle variations in several M5 RR Lyrae stars. We saw no evidence in our data of this effect in any of the four stars in M5 which we analyzed in detail.

The spectroscopic data are from the nights of 1985 April 28 to May 1, 1986 April 15–18 and 1986 May 14–17 at the 200 inch Hale telescope at Palomar Mountain. Integrations were always 30 minutes long as a compromise between avoiding excessive blurring in phase and securing an adequate signal level for high-precision velocities from stellar spectra of low-metallicity stars with few strong spectral features. Observations were carried out irrespective of seeing, transparency, and airmass (within the range up to 2.1 airmasses and absorption due to clouds of less than 1.5 mag). During the 1985 nights, only the largest amplitude RR Lyrae M5-32 was observed. The first two nights' spectra were taken at the 36 inch (91 cm) camera at the coudé focus of the 200 inch (5 m) Hale telescope using a 800×800 TI CCD as a detector. The resolution was 0.14 \AA per pixel. The spectra covered the range 5150–5260 \AA , so that the strongest spectral lines are the Mg triplet. Because the image slicers were not working properly, the signal level was rather low, and for the only remaining usable night in 1985 we switched to the red camera (only) of the Double Spectrograph (again with an 800×800 TI CCD detector). Although this spectrograph was not designed for high-resolution work, by using it in a nonstandard mode with a 1200 g mm^{-1} grating in second order (with substantial vignetting occurring within the optical train), a spectral resolution of 0.37 \AA per pixel can be obtained. With a $1''$ slit, the FWHM of arc lines is 2 pixels. The spectral coverage extended from 5100 to 5400 \AA , including the Mg triplet, and various strong Fe-dominated blends such as 5270 \AA . Typical count rates were 400 electrons per pixel (near maximum light) at the coudé and about 3000 electrons per pixel (near maximum light) at the Double Spectrograph for conditions near $1''$ seeing. During this night the spectrograph was rotated so that the slit rotated to a position angle 14° from the nominal east-west orientation (where flexure is minimized) to include the giant M5-IV-82 (in the numbering system of Arp 1962) as well as M5-32 along the slit. This star was of comparable brightness in the B filter to the M5 RR Lyrae variables at maximum light.

During the first 1986 run, the Double Spectrograph was

used in the same configuration, but the spectrograph was rotated so that the slit was 16° from the east-west line so as to pass through two RR Lyrae variables simultaneously, M5-32 and M5-8. (The Double Spectrograph was designed for use as a long-slit instrument, and with the present CCD detector, the allowed slit length exceeds $2'$, but the maximum slit length visible on the television guiding system is about $85''$. At least three pairs of RR Lyrae variables can be found within M5 that are less than $85''$ apart.) The weather was poor during that run, and a $2''$ slit had to be used. The second 1986 run we alternated between a slit position angle which allowed simultaneous spectra of M5-8 and of M5-32 and a second position angle which allowed simultaneous spectra of the variables M5-12 and M5-59. The rotation in position angle between the two settings was 20° . Noble gas arcs were always taken before and after each exposure in the correct slit orientation. These observations were carried out with phase tables at hand to allow optimum choice of the pair of variables to be observed at any time in order to maximize phase coverage over the entire period for the four stars.

On those nights during which the Double Spectrograph was in use, several bright template stars were observed each night, as well as giants in M3 and M92 (exposed to a signal level similar to that expected for the M5 RR Lyrae stars), all of whose radial velocities are well known. Fewer template stars, and no additional globular cluster giants, were observed while the coudé was used.

The data were reduced using the image processing VAX 11/780 computer of the astronomy department at Caltech. After flattening, the single spectrum or pair of spectra (as well as a sky spectrum chosen from a clean region as free of stars as possible along the slit immediately adjacent to each object), was extracted to one dimension. Next we subtracted off the appropriate sky spectrum. The spectra were cross-correlated with the template spectrum for each night. The arcs were also cross-correlated with the arc for the template star, arcs before each exposure and afterward being treated separately. This enabled the construction of a flexure table as a function of time during each night. For the coudé data, the flexure was negligible. It was quite small for the Double Spectrograph data when the slit was left close to its normal east-west orientation (i.e., not altering the slit position angle during the night), but reached significant values (up to 1 pixel at extreme airmasses) during the last run when the slit was rotated repeatedly during the night. The cross-correlation peaks, signal levels, and visual appearance of the Mg triplet of all the spectra were examined, and several radial velocities were rejected as unreliable. In

general, these were from the beginning or end of the night, when the airmass approached 2.1, and the seeing deteriorated, so the signal level obtained in the maximum 30 minute integration was inadequate. (This was done prior to constructing the radial velocity-phase curves.) The zero point of our radial velocities assumes that the heliocentric radial velocity of μ Leo is 13.86 km s^{-1} and that of HD 122563 is -24.7 km s^{-1} . (These are the mean values for the modern determinations in Abt and Biggs 1972.)

The radial velocities of the M3 stars were compared with those of Gunn and Griffin (1979), and their repeatability from night to night was also examined. The rms deviation about our mean velocity for the three M3 stars observed repeatedly was 4 km s^{-1} . The comparison with the published radial velocities revealed differences in our mean versus those of Gunn and Griffin with a total range of only 2.7 km s^{-1} once a constant zero point difference was removed. We also note that the rms variation about the mean of our 13 radial velocity measurements for M5-IV-82 was only 1.2 km s^{-1} , although admittedly this star is somewhat brighter than the M5 RR Lyrae stars. We therefore assess the uncertainties of our radial velocities from coude spectra as 3 km s^{-1} , and from the Double Spectrograph observations as 4 km s^{-1} .

The heliocentric radial velocities derived from the spectra are listed in Table 2 as a function of Julian day and phase within the period for the 4 RR Lyrae variables in M5. The time and phase are given for the midpoint of the 30 minute exposures. There are 28, 30, and 31 independent radial velocities respectively for M5-8, 12, and 59, while for M5-32 (the only star observed in both 1985 and 1986) we have 56 independent radial velocity measurements. The radial velocity-phase (ϕ) curves are plotted for the four stars in Figure 1. The 1986 data are indicated by filled points, while the 1985 data are shown as crosses. The effort to achieve full phase coverage was reasonably successful; only M5-8 has an interval in ϕ as large as 0.1 cycles within which there is no accepted radial velocity measurement. Smooth curves were drawn through the v_r - ϕ curve for each star, and the mean velocities (v_r) were determined. These are 48.0, 53.1, 51.2, and 49.4 km s^{-1} , respectively, for the RR Lyrae variables M5-8, 12, 32, and 59. Several different hand-drawn curves which might seem to fit the points for a given star acceptably were tried; the resulting change in v_r was always less than 1.2 km s^{-1} . Note that the radial velocity for M5 compiled by Webbink (1981) is 51.9 km s^{-1} .

b) Photometric Data

Ideally one desires spectrophotometry covering the entire optical spectral bandpass of the RR Lyraes in M5 which extends over the complete cycle. Although several nights of such data were obtained with the 60 inch (1.5 m) telescope at Palomar Mountain, using a spectrograph with a 6" slit and a CCD detector, the data were never used because crowding problems in the globular cluster fields prevent one from achieving the necessary accuracy. Instead we resorted to photometry as measured from direct CCD images through wide-band filters. In order to get the maximum possible leverage on temperature variations over the cycle, the filters chosen were the Johnson B filter and a near-infrared i filter adopted for use with CCDs which reproduces the system of Wade *et al.* (1979) (see also Schneider, Gunn, and Hoessel 1983; Thuan and Gunn 1976). The direct imaging CCD system at the Palomar 60 inch was used to obtain photometry during the five nights of 1986 May 28 through June 1. The first three of these nights were

photometric; the last two were quite cloudy at times. The seeing varied between $1''$ and $2''$ over the five nights, except when it was extremely cloudy.

An RCA 320×512 CCD was used mounted at the Cassegrain focus of the 60 inch telescope. The scale was $0''.46$ per pixel. This meant that the four variables for which radial velocity data had been obtained could not be covered in a single exposure, and two fields were necessary. Within the first field, centered near M5-8 and M5-32, were also located the RR Lyrae stars M5-18, 19, 28, and 31. The second field was centered near M5-12 and M5-59, and also included the RR Lyrae M5-79. The exposures were unguided and were 2 minutes through the B filter and 30 seconds through the i filter when it was clear. Frames through each of the two filters were obtained for the first field; then the second field was observed. Except for interruptions due to standard stars and an attempt to confirm a possible supernova, this continued as long as M5 was higher than 2.0 airmasses. Because not all the nights were photometric, local standards were set up within each frame and used to calibrate the data from the last two nights of poor and variable transparency. Occasionally during these two nights, the transparency was so poor that no observing was possible, or when the transparency improved somewhat, only i measurements were made. Some of the frames on these two nights were integrations up to 6 minutes long in B and 200 s in i .

The standard stars of the Thuan-Gunn (1976) system were observed repeatedly throughout the photometric nights. These stars also have well-determined B magnitudes, and they define the zero point of our magnitude system. For the M5 RR Lyrae stars, an aperture photometry code with apertures of 5 pixels in radius ($2''.3$) was used to determine magnitudes from the flattened CCD frames. For the most crowded stars, M5-79 and M5-59, an aperture 3 pixels in radius ($1''.4$) was used. (The differential crowding correction between an aperture whose radius was 3 pixels versus 5 pixels was up to 0.1 mag for these two stars.) Aperture corrections to large apertures were derived from the most isolated bright stars on each frame. On the photometric nights, the corrections from the small-aperture measurements onto the magnitude scale set by the local standards clearly showed the effects of deteriorating seeing and transparency when M5 was far from culmination.

The raw data on the photometric nights are extremely good, with more than 10^4 detected electrons above the level of the sky over the stellar image of the RR Lyraes at all phases. The accuracy of the photometry from the last two nights is significantly worse. Other factors which may cause an occasional bad magnitude are cosmic-ray hits, although these were eliminated when we noticed them on the image of a variable, and the variable lying superposed on the single bad column in the detector. This last problem is more serious in the B frames than in the i frames, as the brighter sky in the latter tended to fill in the bad column to some extent. The B and i magnitudes, together with the Julian date of the mean time of the B and i frame, are listed in Table 3A for the field including M5-12 and M5-59, and in Table 3B for the second field. They are plotted as a function of phase in Figure 2. There are about 90 pairs of measurements for each variable, except M5-19, which was often close to the edge of the field and sometimes completely off the edge of the frames.

These B and i magnitudes were transformed to V magnitudes using the relationship

$$V = B - 0.519(B - i) - 0.293,$$

TABLE 2
RADIAL VELOCITIES OF M5 RR LYRAE STARS

M5-8			M5-12			M5-32			M5-59		
Julian Date -2446000	Phase	V_r (km s^{-1})	Julian Date -2446000	Phase	V_r (km s^{-1})	Julian Date -2446000	Phase	V_r (km s^{-1})	Julian Date -2446000	Phase	V_r (km s^{-1})
538.898	0.381	49.4	565.653	0.334	44.0	184.749	0.436	53.1	565.653	0.249	31.5
538.922	0.424	50.3	565.677	0.384	53.8	184.771	0.483	60.6	565.677	0.293	39.5
538.945	0.467	55.3	565.699	0.432	51.5	184.799	0.544	64.7	565.699	0.334	41.7
538.992	0.554	59.2	565.720	0.476	56.0	184.823	0.597	60.2	565.720	0.372	45.4
539.739	0.921	47.1	566.674	0.515	66.0	184.845	0.645	72.3	566.694	0.170	30.2
539.763	0.965	23.3	566.697	0.564	73.6	184.867	0.693	78.3	566.697	0.174	33.5
539.786	0.007	18.4	566.719	0.613	77.8	186.740	0.784	71.2	566.719	0.216	38.1
539.810	0.052	21.5	566.742	0.662	76.8	186.762	0.832	71.5	566.742	0.258	41.4
539.834	0.095	20.7	566.765	0.709	81.2	186.785	0.882	72.9	566.765	0.299	42.6
539.857	0.137	27.8	566.788	0.758	77.9	186.807	0.931	81.1	566.788	0.342	47.3
539.880	0.179	22.2	566.810	0.806	76.2	186.828	0.978	25.6	566.810	0.383	48.5
539.903	0.222	29.1	566.891	0.980	24.0	186.851	0.026	10.1	566.891	0.532	63.4
565.758	0.555	58.1	566.940	0.085	25.0	186.875	0.080	14.6	566.940	0.623	66.1
565.784	0.602	68.4	567.665	0.634	77.9	186.897	0.127	24.9	567.665	0.960	30.5
565.806	0.643	71.4	567.687	0.681	79.1	186.919	0.177	29.9	567.687	0.001	26.0
565.829	0.685	65.6	567.709	0.729	82.9	186.942	0.225	35.2	567.709	0.042	28.0
565.864	0.748	67.5	567.731	0.776	80.6	186.986	0.322	50.6	567.731	0.083	29.3
565.879	0.776	70.7	567.754	0.825	80.6	187.697	0.874	71.4	567.754	0.125	33.0
566.845	0.545	68.7	567.776	0.873	83.6	187.722	0.929	57.9	567.776	0.166	33.2
566.874	0.597	67.4	567.826	0.978	26.4	187.751	0.994	45.2	567.826	0.257	47.3
566.926	0.692	63.1	567.848	0.026	23.2	187.776	0.047	12.9	567.838	0.298	51.2
567.812	0.315	45.6	567.901	0.140	31.8	187.808	0.117	19.1	567.901	0.397	48.0
567.888	0.453	54.0	568.635	0.708	74.7	187.831	0.168	28.0	567.987	0.555	55.3
568.693	0.928	35.0	568.707	0.862	78.3	187.855	0.220	30.7	568.635	0.750	68.5
568.742	0.017	21.0	568.755	0.965	22.8	187.878	0.272	33.5	568.707	0.883	70.2
568.790	0.105	20.4	568.855	0.179	34.4	187.908	0.337	45.8	568.755	0.971	24.5
568.812	0.145	21.2	568.877	0.226	38.8	538.898	0.047	17.8	568.855	0.156	28.0
568.834	0.186	26.1	568.898	0.271	42.0	538.922	0.099	15.8	568.877	0.197	34.8
			568.919	0.317	44.9	538.945	0.150	17.9			
			568.940	0.361	49.8	538.968	0.200	22.5			
						538.992	0.253	22.7			
						539.739	0.884	53.3			
						539.763	0.937	40.0			
						539.786	0.987	15.2			
						539.810	0.040	18.9			
						539.834	0.092	15.7			
						539.857	0.142	16.9			
						539.880	0.192	24.2			
						539.903	0.243	26.2			
						539.937	0.316	35.8			
						565.758	0.721	58.6			
						565.784	0.778	67.8			
						565.829	0.876	64.6			
						565.864	0.952	62.7			
						565.879	0.985	22.7			
						565.925	0.086	7.5			
						566.845	0.096	20.7			
						566.874	0.158	26.3			
						566.926	0.271	32.6			
						567.812	0.207	34.4			
						567.888	0.372	48.0			
						568.693	0.132	25.8			
						568.742	0.238	34.6			
						568.790	0.343	41.5			
						568.812	0.392	47.7			
						568.834	0.440	51.1			

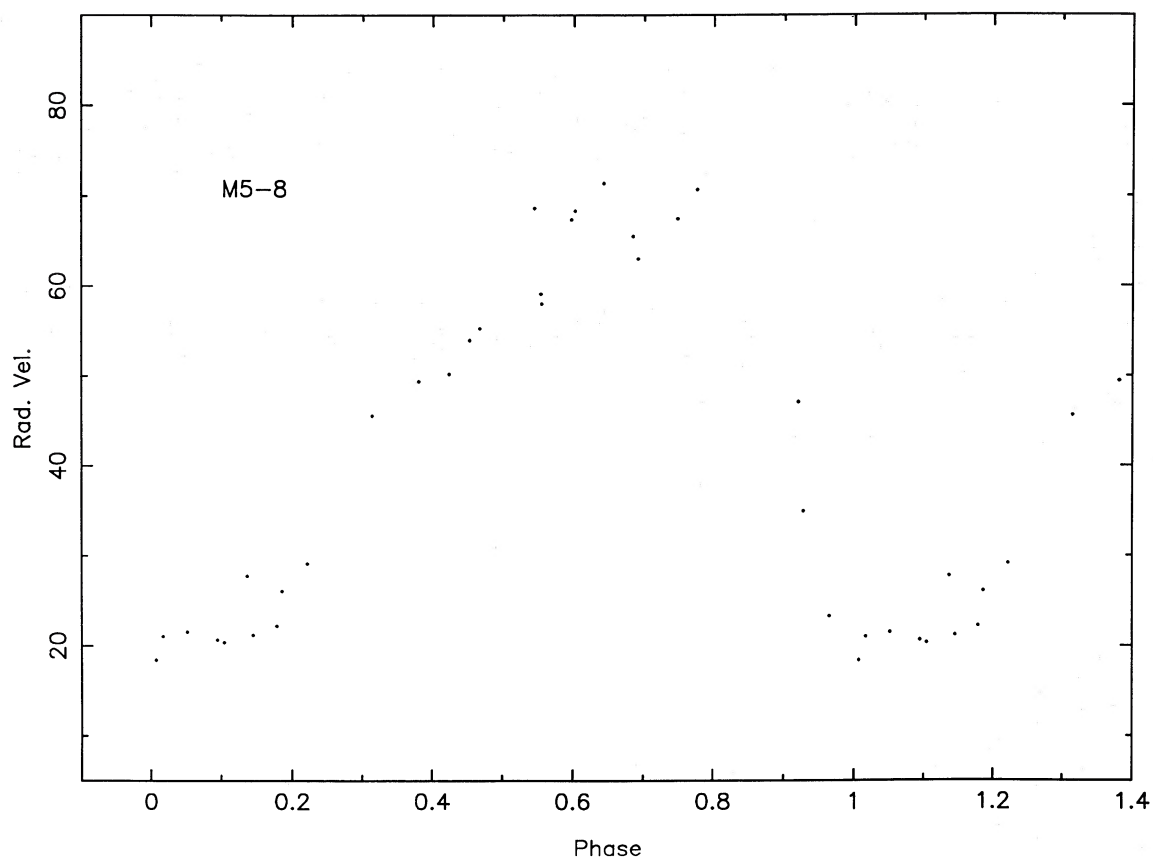


FIG. 1a

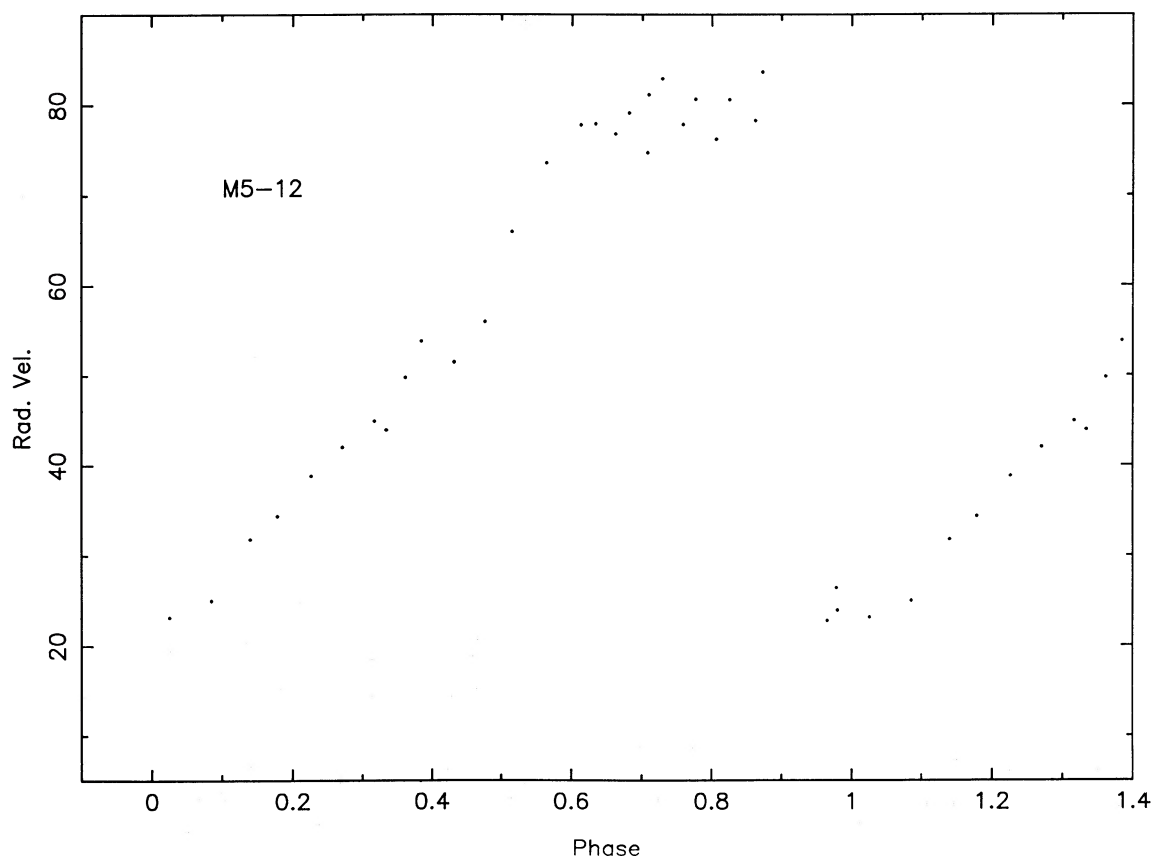


FIG. 1b

FIG. 1.—The radial velocity for the RR Lyrae stars M5-8, M5-12, M5-32, and M5-59 is shown as a function of phase. The points represent the 1986 measurements, while the 1985 measurements for M5-32 are shown by crosses.

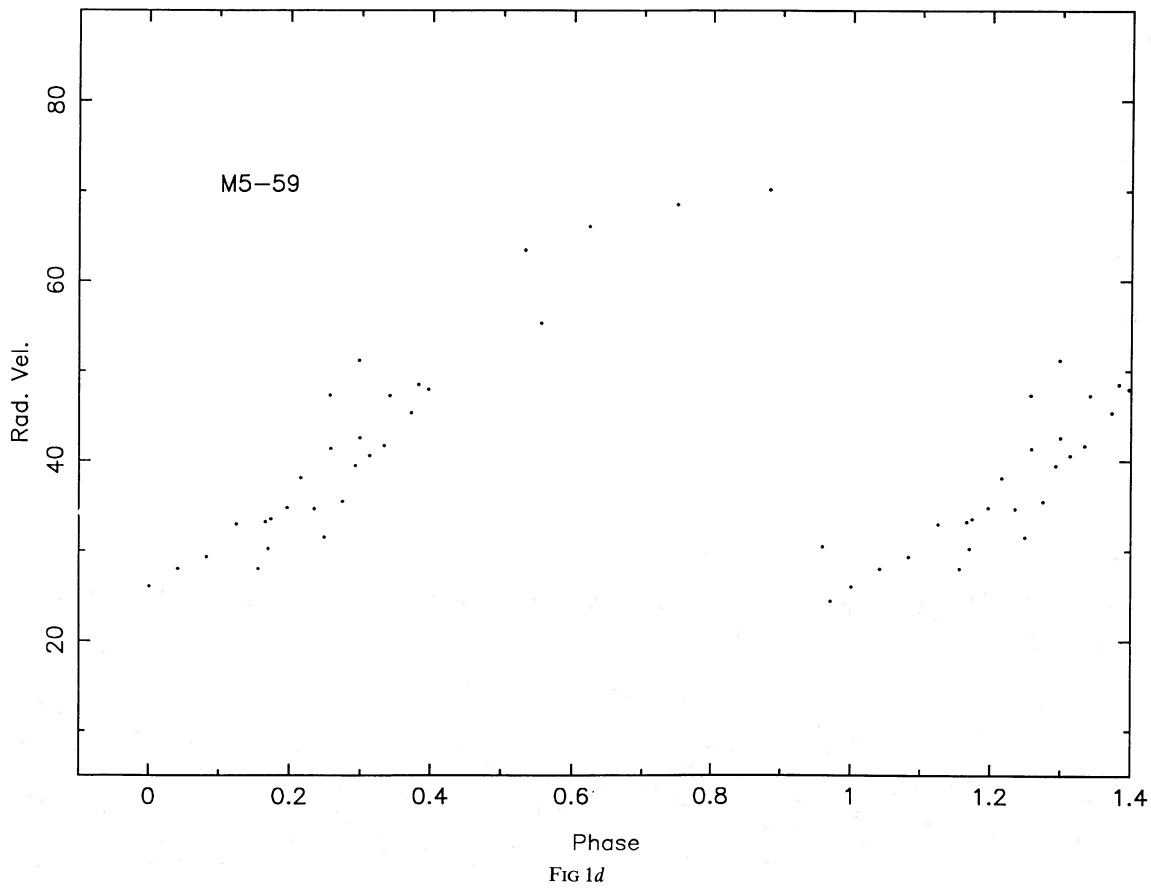
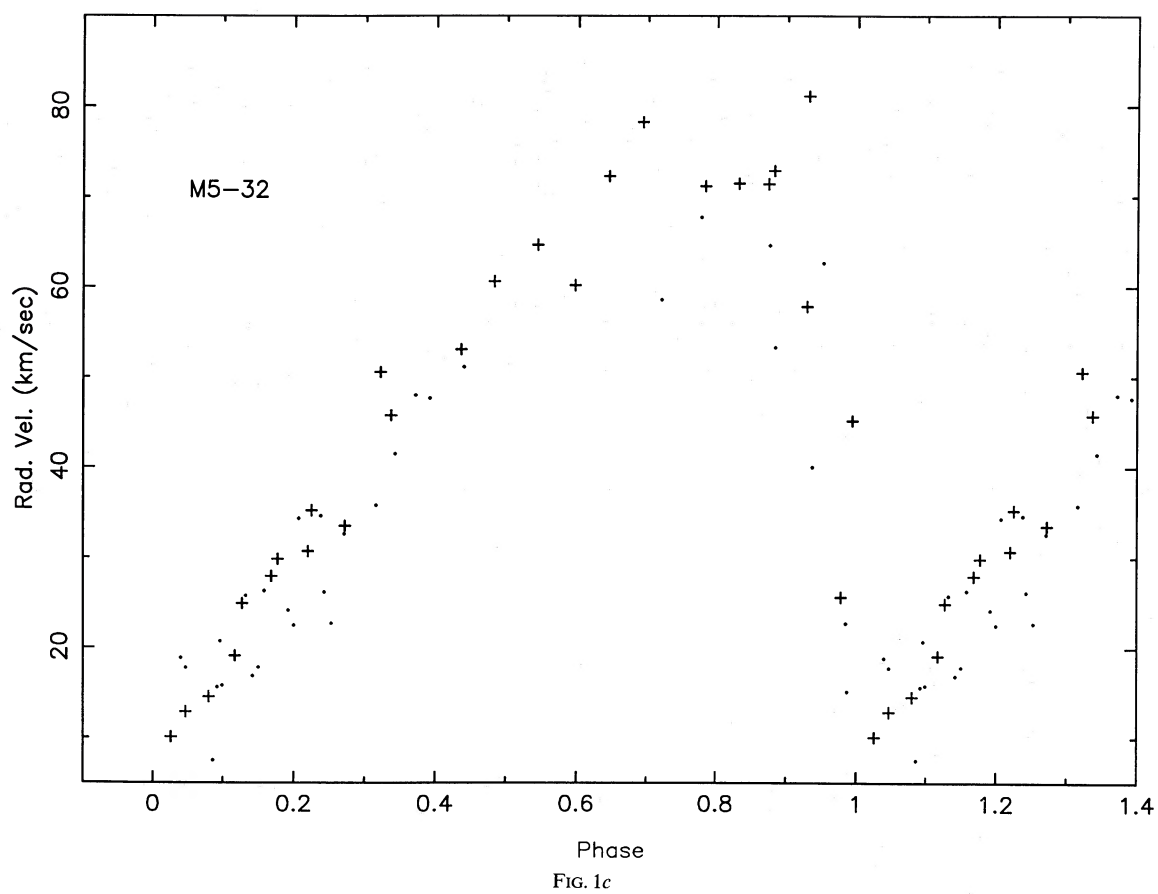


TABLE 3A
 B AND *i* PHOTOMETRY—M5 FIELD 1

Julian Day -2446000	M5-59		M5-12		M5-79		Julian Day -2446000	M5-59		M5-12		M5-79	
	B (mag)	<i>i</i> (mag)	B (mag)	<i>i</i> (mag)	B (mag)	<i>i</i> (mag)		B (mag)	<i>i</i> (mag)	B (mag)	<i>i</i> (mag)	B (mag)	<i>i</i> (mag)
578.669	15.349	15.022	15.081	15.145	15.546	15.250	580.680	14.609	14.813	15.870	15.483	15.405	15.186
578.680	15.393	15.045	15.174	15.188	15.507	15.237	580.701	14.611	14.790	15.939	15.531	15.339	15.175
578.688	15.414	15.067	15.219	15.199	15.453	15.255	580.711	14.668	14.814	15.972	15.549	15.264	15.161
578.705	15.480	15.119	15.338	15.266	15.343	15.194	580.728	14.790	14.890	15.965	15.569	15.190	15.130
578.717	15.531	15.101	15.415	15.292	15.249	15.176	580.742	14.855	14.901	15.972	15.580	15.122	15.084
578.724	15.548	15.127	15.441	15.308	15.213	15.137	580.754	14.926	14.917	15.969	15.585	15.115	15.119
578.733	15.562	15.107	15.501	15.331	15.149	15.088	580.766	15.000	14.962	15.943	15.616	15.057	15.087
578.741	15.591	15.142	15.543	15.326	15.153	15.087	580.776	15.046	14.964	15.959	15.575	15.060	15.042
578.753	15.623	15.157	15.543	15.375	15.095	15.062	580.788	15.120	15.008	15.926	15.615	15.041	15.045
578.778	15.653	15.168	15.717	15.455	15.070	15.049	580.806	15.211	15.009	15.958	15.574	15.071	15.061
578.785	15.687	15.175	15.749	15.434	15.062	15.024	580.820	15.247	15.016	15.957	15.605	15.090	15.069
578.797	15.695	15.197	15.807	15.451	15.062	15.042	580.829	15.294	15.012	15.907	15.653	15.115	15.035
578.804	15.708	15.191	15.829	15.457	15.050	15.052	580.840	15.344	15.057	15.930	15.591	15.176	15.083
578.820	15.716	15.229	15.902	15.488	15.106	15.055	580.855	15.367	15.057	15.973	15.629	15.203	15.105
578.828	15.713	15.199	15.920	15.503	15.125	15.064	581.668	15.808	15.332	16.007	15.531	15.422	15.225
578.844	15.727	15.219	15.956	15.537	15.199	15.108	581.690	15.859	15.336	16.004	15.659	15.361	15.163
578.854	15.724	15.217	15.975	15.548	15.231	15.108	581.726	15.635	15.337	15.922	15.576	15.141	15.078
578.868	15.719	15.265	15.946	15.542	15.323	15.150	581.747	15.058	15.060	15.942	15.620	15.094	15.086
578.880	15.712	15.243	15.931	15.547	15.339	15.214	581.764	14.707	14.852	15.883	15.507	15.116	15.078
578.890	15.759	15.225	15.932	15.604	15.405	15.206	581.781	14.618	14.814	15.959	15.634	15.116	15.095
578.900	15.744	15.243	15.936	15.579	15.438	15.184	581.803	14.743	14.842	16.027	15.709	15.088	15.057
578.912	15.750	15.243	15.971	15.573	15.499	15.222	581.818	14.825	14.878	15.957	15.690	15.075	15.053
578.920	15.735	15.293	15.936	15.569	15.519	15.217	581.833	14.923	14.889	15.624	15.540	15.145	15.053
579.653	14.849	14.860	15.414	15.325	15.531	15.217	581.851	15.011	14.954	14.653	15.073	15.182	15.074
579.663	14.917	14.897	15.493	15.291	15.525	15.266	581.860	15.082	14.995	14.424	14.920	15.232	15.115
579.670	14.947	14.936	15.506	15.311	15.506	15.240	581.871	15.115	14.975	14.408	14.904	15.327	15.159
579.688	15.033	14.967	15.585	15.363	15.435	15.212	581.880	15.173	15.014	14.483	14.931	15.336	15.121
579.695	15.127	14.980	15.619	15.386	15.386	15.196	581.889	15.226	14.986	14.581	14.924	15.375	15.158
579.714	15.169	14.982	15.697	15.407	15.253	15.146	581.907	15.261	15.037	14.724	15.020	15.447	15.217
579.721	15.207	14.999	15.728	15.450	15.214	15.141	581.916	15.318	15.040	14.812	15.072	15.461	15.220
579.743	15.310	15.027	15.854	15.487	15.182	15.112	582.649	15.858	15.252	15.795	15.541	15.567	15.289
579.752	15.332	15.047	15.871	15.481	15.139	15.097	582.661	15.741	15.230	15.905	15.596	15.512	15.246
579.774	15.415	15.065	15.931	15.512	15.015	15.036	582.667	15.733	15.231	15.941	15.581	15.519	15.234
579.783	15.463	15.072	15.973	15.539	14.999	15.029	582.685	15.711	15.253	15.931	15.585	15.400	15.220
579.799	15.491	15.083	15.968	15.516	15.022	15.034	582.697	15.787	15.312	15.968	15.527	15.317	15.138
579.806	15.526	15.113	15.967	15.558	15.065	15.039	582.712	15.748	15.214	15.970	15.612	15.210	15.122
579.819	15.572	15.118	15.881	15.539	14.989	15.045	582.726	15.720	15.236		15.628	15.307	15.054
579.830	15.605	15.136	15.962	15.573	15.154	15.047	582.769		15.363		15.429		15.072
579.846	15.659	15.134	15.949	15.585	15.225	15.099	582.784	15.854	15.352	14.654	15.119	15.126	15.048
579.860	15.684	15.185	15.964	15.571	15.283	15.116	582.811	15.645	15.296	14.471	14.899	15.109	15.013
579.874	15.687	15.178	15.957	15.574	15.339	15.140	582.831	15.120	15.024	14.645	14.979		15.078
579.896	15.724	15.207	15.940	15.591	15.425	15.188	582.839	15.005	14.961	14.725	15.026	15.159	15.089
579.902	15.717	15.190	15.953	15.613	15.429	15.186	582.847	14.822	14.849	14.797	15.043	15.210	15.120
579.913	15.720	15.191	15.988	15.574	15.485	15.183	582.856	14.637	14.825	14.873	15.095	15.256	15.152
579.920	15.729	15.221	16.050	15.684	15.508	15.230	582.862	14.584	14.792	14.921	15.079	15.258	15.128
580.657	15.113	15.087	15.746	15.452	15.473	15.264							
580.668	15.078	14.981	15.795	15.442	15.469	15.202							
580.675	14.893	14.891	15.825	15.456	15.468	15.222							

which was derived from bright standard stars covering a range in $B-i$ color which exceeded 2.7 mag. For each variable, the V magnitudes were averaged over the cycle (in bins of 0.02 in ϕ) to determine the mean V color, and were converted to intensities, then averaged over the cycle, then converted back to a magnitude, to yield the intensity mean V magnitude. These parameters, together with the minimum and maximum of the light curves in B , i , and V , are listed in Table 1. An interstellar absorption correction at V of 0.093 mag has been adopted for M5 (Zinn 1980).

III. DERIVATION OF DISTANCES AND MEAN RADII

a) Method of Analysis

The analysis of this data has as its goal the derivation of the angular diameter (henceforth θ) as a function of phase from both the radial velocity and the photometric data sets. Forcing agreement between these two $\theta(\phi)$ relationships determines the

distance to the pulsating variable star. The manipulation of the radial velocities is straightforward. A hand-drawn curve which fits the radial velocity- ϕ relationship for each M5 RR Lyrae was digitized at 0.02 cycle intervals. The pulsational velocity is the difference between v_r and the mean velocity v_r , defined in § IIa, multiplied by the projection factor p to convert a line-of-sight velocity into a pulsational velocity. This factor has been set at 1.31. Values adopted in recent analyses in the literature range from 1.30 to 1.35; the choice of p and the accuracy to which it is known are discussed in Hindsley and Bell (1986). If p is underestimated by 5%, the distance to the pulsating variable star will be underestimated by 5%.

The pulsational velocity is then integrated over time (i.e., phase \times the period of the variable) to yield the difference in radius $\delta R(\phi)$. The integration is straightforward and has been checked by reproducing the results of Oke (1966) from the v_r - ϕ curve for the field RR Lyrae star X Ari. We begin the integration just past maximum light when the star begins to expand,

as that puts the worst determined part of the pulsational velocity curve, that of the rapid drop in radial velocity at maximum light, at the end of the integration. If a value for the radius at $\phi = 0$ and one for the distance to M5 are assumed, the angular diameter over the cycle is easily obtained.

Ideally we want to measure a radial velocity from a spectral feature arising at the same optical depth where the continuum is formed; this is clearly impossible. We have used the Mg triplet region, which in these metal-poor stars contains only relatively weak absorption lines. However, one might be concerned, should a strong gradient in pulsational velocity with depth exist, that the varying depth of line formation for a given spectral feature (due to the varying T_{eff} with phase) as a function of phase could lead to a radial velocity curve which does not follow the pulsational velocity. Fortunately Jones *et al.* (1987a) have already demonstrated that the velocity gradient with depth, at least over the relevant range of optical depth, is small. We are thus confident that the observed radial velocity

curve is a true reflection of the pulsational velocity as a function of phase.

The derivation of the θ - ϕ relationship from the photometric data is more complex, and several different schemes have been applied in the literature. We have developed an independent analysis which has the advantage that the sources of uncertainty are much more clearly visible. We have measured $B-i$ colors as a function of phase. We use the grid of models of Kurucz (1979), adopting $Z/Z_0 = 1/10$. (Frogel, Cohen, and Persson 1983 deduced $[\text{Fe}/\text{H}](\text{M5}) = -1.5$ dex, while Zinn and West 1984 derived -1.4 dex. The error introduced by not interpolating properly within the Kurucz grid between models of 0.1 and 0.01 solar metallicity is discussed in § IVa and is not significant.) These models are used setting the effective wavelength of the B filter as 4512 Å and that of the i filter as 8050 Å to define the dependence of the $B-i$ color on T_{eff} and surface gravity. The zero point of the $B-i$ colors is fixed by the analysis of Bell and Oke (1986) of the bright metal-poor sub-

TABLE 3B
B AND i PHOTOMETRY—M5 FIELD 2

Julian Day -2446000	M5-32		M5-8		M5-19		M5-31		M5-28		M5-18	
	B (mag)	i (mag)	B (mag)	i (mag)	B (mag)	i (mag)	B (mag)	i (mag)	B (mag)	i (mag)	B (mag)	i (mag)
578.675	15.599	15.398	15.339	15.232			15.681	15.547	15.395	15.210	15.052	15.156
578.685	15.044	15.140	15.367	15.213			15.674	15.580	15.446	15.199	15.131	15.162
578.691	14.674	14.951	15.420	15.265			15.679	15.575	15.487	15.241	15.166	15.179
578.710	14.419	14.868	15.454	15.233			15.667	15.576	15.533	15.215	15.311	15.223
578.721	14.456	14.896	15.491	15.231			15.659	15.575	15.552	15.251	15.366	15.243
578.737	14.626	14.978	15.555	15.275			15.609	15.527	15.603	15.278	15.464	15.284
578.750	14.745	15.036	15.597	15.268			15.465	15.471	15.630	15.255	15.524	15.309
578.758	14.824	15.065	15.625	15.278			15.338	15.404	15.649	15.277	15.555	15.333
578.779	15.057	15.124	15.710	15.333			15.059	15.289	15.744	15.288	15.657	15.355
578.789	15.131	15.176	15.734	15.327	16.068	15.626	15.098	15.324	15.778	15.329	15.675	15.330
578.801	15.211	15.227	15.777	15.338	16.044	15.644	15.065	15.256	15.773	15.341	15.716	15.403
578.808	15.259	15.249	15.784	15.338	15.908		15.055	15.290		15.313	15.722	15.420
578.824	15.390	15.257	15.862	15.368		15.636	15.022	15.240	15.873	15.367	15.748	15.413
578.833	15.401	15.295	15.841	15.391	16.028	15.643	15.028	15.279	15.827	15.373	15.747	15.417
578.848	15.523	15.332	15.850	15.427		15.645	15.088	15.277		15.360	15.770	15.442
578.858	15.541	15.366	15.889	15.410	15.968		15.102	15.286	15.844	15.368	15.752	15.429
578.872	15.629	15.401	15.897	15.454	15.970	15.627	15.192	15.432	15.871	15.431	15.786	15.487
578.883	15.735	15.407	15.946	15.455	16.022	15.621	15.315	15.425	15.898	15.416	15.872	15.459
578.892	15.718	15.439	15.909	15.449	15.975	15.660	15.303	15.487	15.844	15.419	15.825	15.493
578.906	15.814	15.447	15.883	15.424	15.993	15.684	15.425	15.483	15.883	15.428	15.820	15.482
578.915	15.822	15.482	15.893	15.458	15.869	15.617	15.437	15.549	15.839	15.408	15.799	15.462
578.924	15.852	15.485	15.897	15.479	15.621	15.513	15.454	15.450	15.854	15.505	15.784	15.465
579.660	14.698	15.024	14.670	14.913	15.921	15.557	15.381	15.442	14.817	14.973	15.410	15.297
579.667	14.790	15.064	14.705	14.939	15.934	15.540	15.253	15.349	14.858	15.013	15.483	15.399
579.675	14.850	15.090	14.749	14.964	15.964	15.534	15.152	15.303	14.920	15.016	15.560	15.401
579.692	15.005	15.149	14.852	15.016	15.893	15.609	15.105	15.342	15.002	15.035	15.567	15.310
579.698	15.080	15.159	14.892	15.014	16.019	15.580	15.111	15.306	15.053	15.046	15.608	15.371
579.717	15.224	15.246	15.016	15.063	16.044	15.624	15.028	15.254	15.146	15.098	15.681	15.374
579.725	15.270	15.264	15.053	15.082	16.047	15.624	15.008	15.226	15.205	15.124	15.700	15.396
579.747	15.412	15.303	15.193	15.113	16.034	15.614	15.067	15.273	15.290	15.141	15.736	15.423
579.756	15.464	15.337	15.235	15.130	16.043	15.675	15.099	15.298	15.343	15.142	15.728	15.416
579.778	15.585	15.360	15.328	15.160	16.028	15.644	15.181	15.329	15.454	15.194	15.729	15.266
579.788	15.622	15.372	15.382	15.198	16.011	15.635	15.250	15.352	15.487	15.217	15.565	15.449
579.803	15.687	15.418	15.448	15.216	15.967	15.623	15.350	15.439	15.537	15.227	15.776	15.363
579.810	15.723	15.446	15.486	15.191	15.957	15.630	15.295	15.497	15.552	15.239	15.782	15.496
579.824	15.798	15.476	15.550	15.245	15.977	15.651	15.430	15.450	15.623	15.280	15.836	15.493
579.835	15.844	15.499	15.577	15.257	15.998	15.653	15.511	15.488	15.647	15.282	15.847	15.506
579.850	15.880	15.522	15.647	15.331	15.912	15.578	15.584	15.480	15.702	15.292	15.816	15.603
579.865	15.951	15.545	15.679	15.298	15.622	15.434	15.649	15.536	15.742	15.315	15.879	15.591
579.878	15.984	15.553	15.730	15.332	14.907	15.091	15.684	15.558	15.785	15.349	15.873	15.533
579.899	15.965	15.551	15.779	15.347	14.396	14.838	15.675	15.563	15.833	15.348	15.877	15.586
579.906	15.947	15.554	15.795	15.344	14.418	14.872	15.703	15.558	15.821	15.379	15.861	15.611
579.917	15.935	15.571	15.813	15.364	14.496	14.926	15.718	15.671	15.843	15.368	15.843	15.557
580.664	15.424	15.289	16.030	15.562	16.044	15.626	15.109	15.284	15.955	15.536	15.736	15.439
580.671	15.430	15.289	16.015	15.570	16.022	15.641	15.148	15.293	15.850	15.491	15.836	15.571
580.679	15.484	15.271	16.013	15.604	16.021	15.659	15.203	15.296	15.695	15.455	15.822	15.498
580.691	15.555	15.329	15.925	15.498	16.020	15.587	15.274	15.482	15.282	15.134	15.759	15.429
580.696	15.593	15.349	15.879	15.523	16.017	15.606	15.306	15.467	15.170	15.153	15.773	15.449

TABLE 3B—Continued

Julian Day -2446000	M5-32		M5-8		M5-19		M5-31		M5-28		M5-18	
	B (mag)	i (mag)	B (mag)	i (mag)	B (mag)	i (mag)	B (mag)	i (mag)	B (mag)	i (mag)	B (mag)	i (mag)
580.716	15.780	15.458	15.395	15.240	15.964		15.383	15.444	14.801	14.952	15.759	15.426
580.724	15.705	15.404	15.130	15.155	16.036	15.648	15.446	15.542	14.716	14.917	15.883	15.446
580.739	15.763	15.447	14.787	14.995	15.975	15.632	15.540	15.481	14.765	14.939	15.875	15.637
580.750	15.806	15.497	14.679	14.942	15.941	15.626	15.597	15.522	14.840	14.964	15.916	15.622
580.762	15.841	15.552	14.719	14.947	15.971	15.645	15.650	15.528	14.911	15.024	15.813	15.632
580.773	15.910	15.511	14.792	14.967	15.966	15.608	15.668	15.531	14.990	15.017	15.889	15.582
580.793	15.928	15.537	14.900	15.017	15.848	15.592	15.712	15.585	15.093	15.047	15.847	15.513
580.810	15.934	15.570	15.026	15.066		15.268	15.672	15.567	15.195	15.118	15.884	15.567
580.816	15.943	15.548	15.056	15.081	14.909	15.176	15.649	15.569	15.231	15.139	15.930	15.581
580.826	15.920	15.563	15.123	15.096	14.537	14.963	15.648	15.550	15.272	15.137	15.945	15.695
580.837	15.911	15.575	15.178	15.121	14.441	14.877	15.610	15.561	15.302	15.139	15.981	15.600
580.855	15.894	15.570	15.262	15.152	14.520	14.926	15.475	15.474	15.415	15.181	15.844	15.514
581.683	15.825	15.564		15.328	15.943	15.653	15.655	15.405	16.101	15.542	15.905	25.152
581.701	15.936	15.562	15.855	15.426	15.929	15.628	15.652	15.531	15.929	15.545	16.041	15.841
581.719		15.528		15.516		15.540				15.619		15.504
581.739	15.930	15.570	15.901	15.519	15.607	15.514	15.619	15.556	15.994	15.541	15.985	15.525
581.756	15.905	15.608	15.963	15.621	15.000	15.030	15.512	15.452	15.913	15.550	15.837	15.620
581.774		15.574	15.919	15.562	14.443	14.897	15.401	15.356	15.595	15.165	15.815	15.525
581.790	15.898	15.566	15.857	15.471			15.051	15.260	15.060	15.027	15.772	15.478
581.813	15.869	15.580	15.274	15.158		15.032	15.047	15.319	14.717	14.921	15.481	15.346
581.823	15.880	15.581	15.000	15.052	14.805	15.060	15.017	15.305	14.721	14.933	15.250	15.245
581.839	15.934	15.646	14.712	14.930	14.958	15.122	15.001	15.345	14.829	14.966	14.887	15.087
581.857	15.987	15.629	14.704	14.921	15.129	15.177	15.098	15.285	14.950	15.053	14.694	14.975
581.865	15.915	15.620	14.740	14.943	15.119	15.249	15.097	15.319	15.006	15.101	14.721	15.060
581.875	15.706	15.438	14.801	14.995			15.151	15.358	15.064	15.086	14.797	15.023
581.885	15.231	15.212	14.874	15.013			15.223	15.350	15.134	15.065	14.848	15.079
581.910	14.387	14.855	15.123	15.054			15.346	15.403	15.354	15.138	15.019	15.115
582.656	15.921	15.573	15.839	15.390	15.907	15.668	15.446	15.499	15.829	15.353	15.853	15.563
582.663	15.912	15.555	15.922	15.434	15.832	15.620	15.377	15.586	15.838	15.392	15.849	15.700
582.671	15.910	15.581	15.893	15.405	15.740	15.538	15.244	15.352	15.874	15.354	15.875	15.502
582.690	15.911	15.534	15.879	15.469	15.271	15.294	15.034	15.242	15.861	15.432	15.882	15.502
582.706	15.962	15.476	15.914	15.438	14.614	14.669	15.080	15.262	15.917	15.497	15.854	15.604
582.721	15.969	15.510	15.830	15.383		14.915	15.057	15.197	15.961	15.447	15.748	15.465
582.764		15.687		15.434		15.096		15.297		15.655		15.127
582.774		15.647		15.422		15.106		15.292		15.404		15.018
582.780		15.658		15.457		15.150		15.299		15.490		15.001
582.794	15.635	15.417	15.867	15.501	15.148	15.200	15.222	15.312	15.949	15.543	14.755	15.035
582.819	14.446	14.869	15.850	15.500		15.259	15.347	15.447	15.943	15.535	14.864	15.099
582.835	14.422	14.876	15.942	15.554			15.448	15.452	15.962	15.510	14.986	15.107
582.843	14.498	14.898	15.957	15.609	15.437		15.519	15.492	15.860	15.449	15.032	15.128
582.850	14.573	14.940	15.986	15.546	15.491	15.311	15.564	15.490	15.754	15.412	15.083	15.155
582.858	14.651	14.997	15.992	15.554	15.518	15.372	15.592	15.515	15.517	15.341	15.129	15.121
582.865	14.710	15.011	15.980	15.595	15.553	15.365	15.625	15.504	15.274	15.216	15.191	15.171

dwarfs that define the Thuan-Gunn system and also serve as spectrophotometric standards. Thus $B-i = 0.40$ mag corresponds to $T_{\text{eff}} = 6000$ K and $\log(g) = 3.7$ (at the metallicity corresponding to the subdwarfs of $Z/Z_{\odot} = 1/100$). This defines our derivation of $T_{\text{eff}}(\phi)$ assuming the surface gravity is known as a function of phase. We begin by assuming that $g(\phi)$ varies as a result of the variation of $R(\phi)$ only (ignoring non-gravitational acceleration). (This is justified in part by considering the relative magnitude of the two accelerations as a function of phase.) We can then assume a mass of $0.6 M_{\odot}$ and take the $R(\phi)$ found by the previous analyses of field RR Lyrae variables, specifically that of Manduca *et al.* (1981), to provide an initial guess for $g(\phi)$. Thus $T_{\text{eff}}(\phi)$ is completely specified.

We proceed by assuming that the calibration of absolute flux from above Earth's atmosphere by Oke and Gunn (1983) is correct. Using 8100 \AA as the effective wavelength for the i filter, we deduce from each observed i magnitude corrected for interstellar absorption the observed flux $f(i)$ in units of $\text{ergs s}^{-1} \text{ cm}^{-2} \text{ Hz}^{-1}$. We assume that the emitted flux at 8050 \AA (F_{8050}) of the Kurucz grid of (static) model stellar atmospheres is correct. Thus F_{8050} is parameterized as a function of T_{eff} and g for the models with metallicity one-tenth the solar value. We

then solve directly for the angular diameter,

$$\theta(\phi) = 2 \sqrt{\frac{f(8100)}{\pi F_{8050} [T_{\text{eff}}(\phi), g(\phi)]}}$$

where the factor of π converts Kurucz's tabulated fluxes to astrophysical fluxes. Thus each pair of B, i magnitudes is transformed into a point on the photometric $\theta(\phi)$ relationship. This calculation is done only once, as the derived $\theta(\phi)$ is completely specified by the observational data, the grid of model atmospheres, and the absolute flux conversion factors.

We can verify the accuracy of this analysis by considering stars with known angular diameters. There are two stars for which θ was measured by Hanbury Brown, Davis, and Allen (1974) which lie in the T_{eff} regime under consideration here. Unfortunately, neither of those has absolute spectrophotometry nor near-infrared i photometry, so that T_{eff} for these test cases cannot be derived from their $B-i$ colors. However, if we use, for example, the results of Dreiling and Bell (1980) for the T_{eff} and surface gravity of α Lyrae, assuming solar metallicity, to predict the star's emitted flux and take its observed flux at 8100 \AA from Oke and Gunn (1983), we deduce $\theta(\text{Vega}) =$

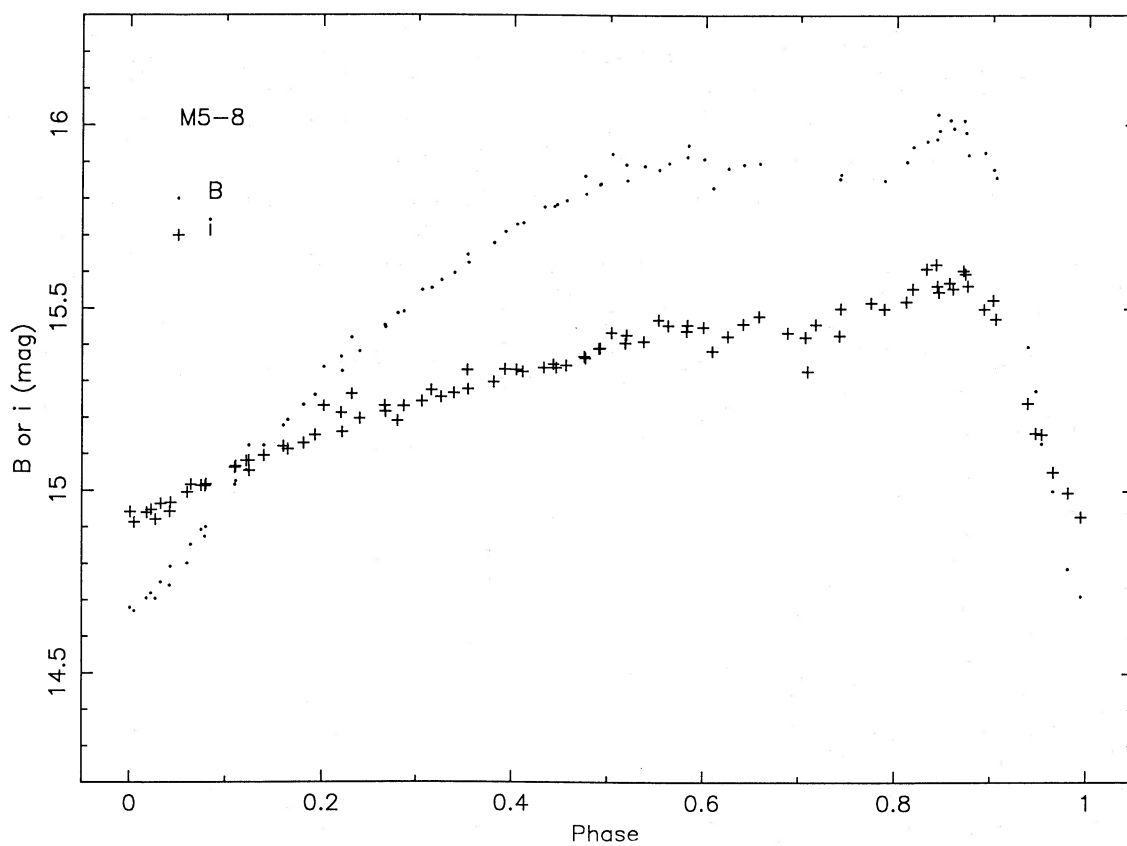


FIG. 2a

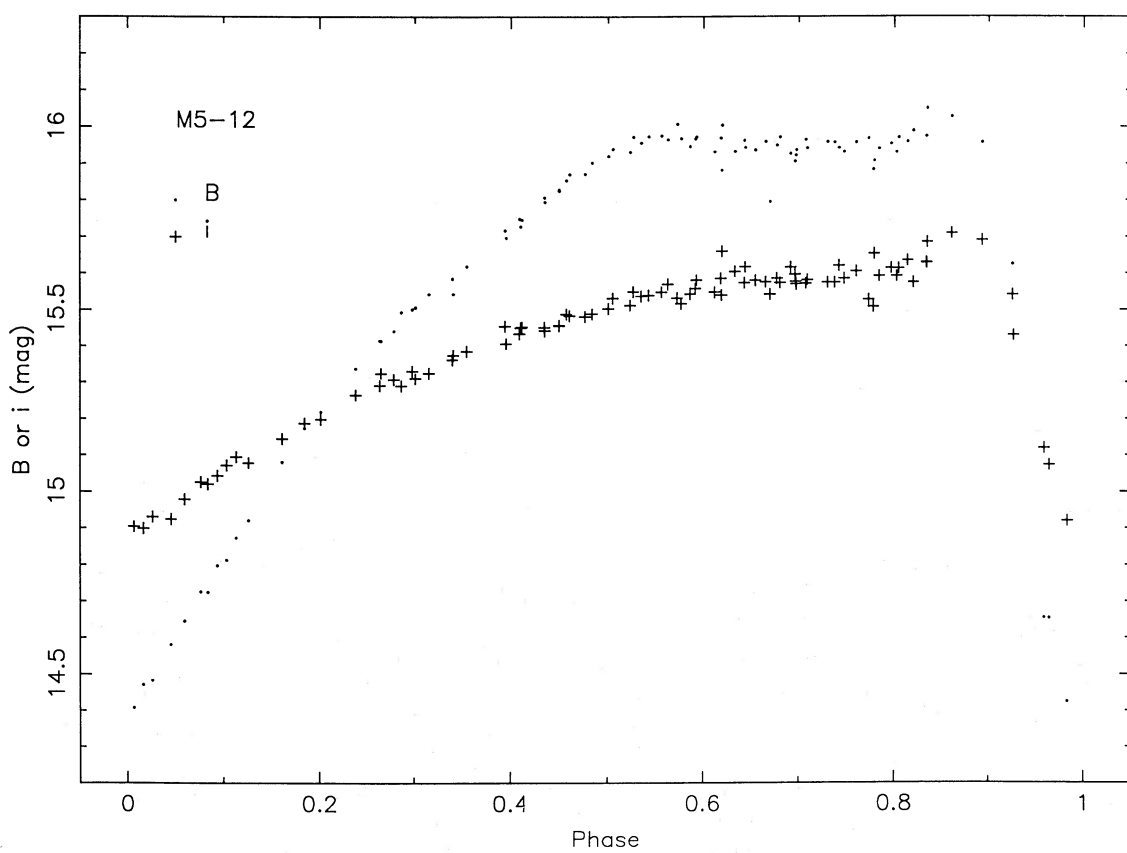


FIG. 2b

FIG. 2.—The *B* (points) and *i* (crosses) light curves for the four RR Lyrae variables in M5 are shown

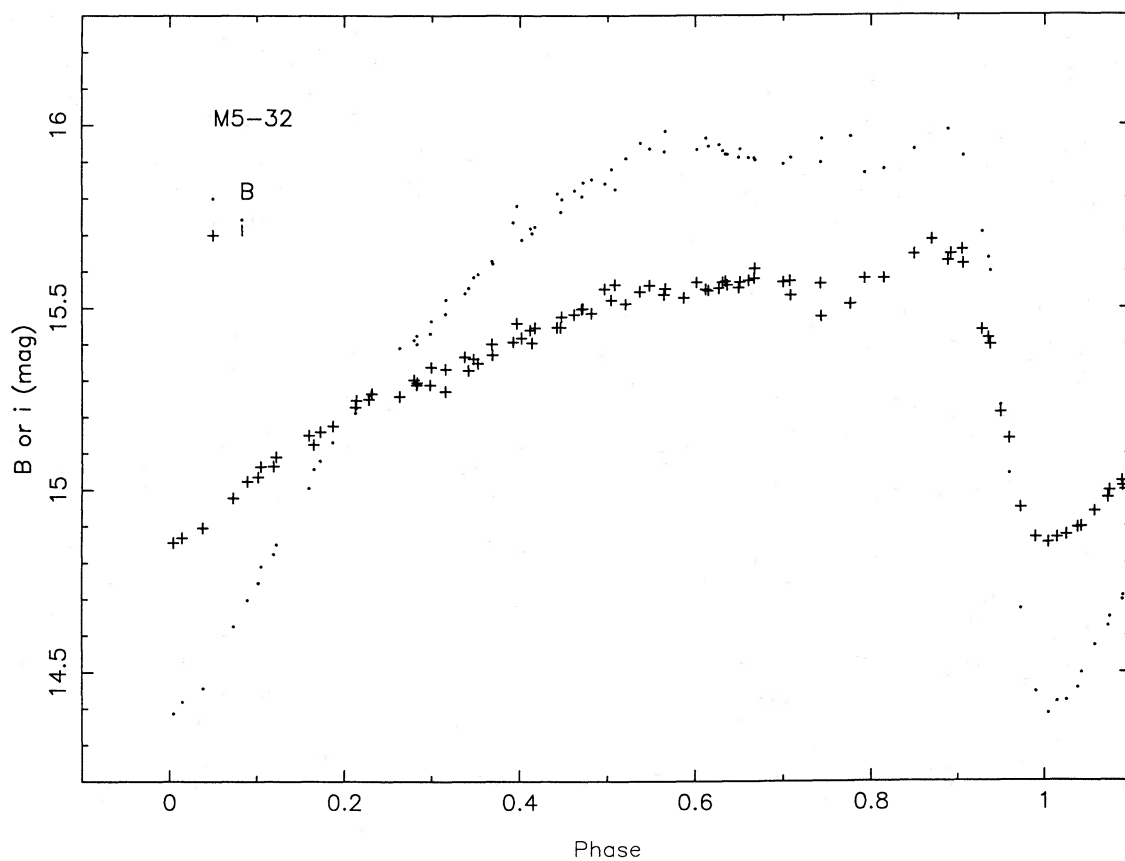


FIG. 2c

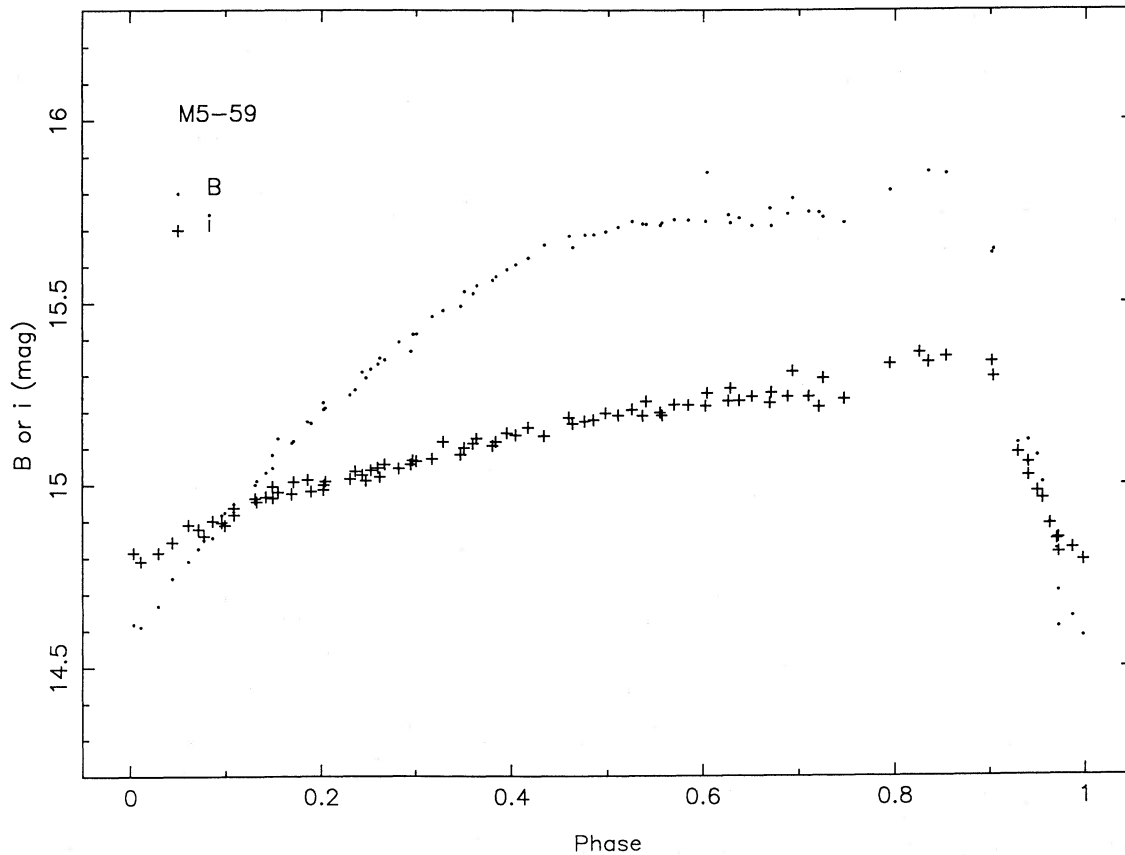


FIG. 2d

0^m.00320, equal to the observed value of $3^{\text{h}}24^{\text{m}} \pm 0^{\text{h}}07^{\text{m}} \times 10^{-3}$ (Hanbury Brown, Davis, and Allen 1974) to within the uncertainty of the measurement.

We now vary the values adopted for the distance and radius at $\phi = 0$ until the two θ - ϕ relationships are in best coincidence. Several fitting routines were written for this purpose. The best value of $R(\phi = 0)$ for a given distance is found by minimizing the sum

$$\sum_{i=1}^N [\theta(\text{phot})_i - \theta(v_r)]$$

over each of the N pairs of B , i magnitudes with both terms evaluated at the phase corresponding to the i th pair. Let us denote the derived best value of $R(\theta = 0)$ for a given distance as R_D . Then we calculate a series of sums for various choices of the distance D . These sums are identical to the first set except that for each choice of D the appropriate value of R_D is adopted and also each term in the sum written above is replaced by its absolute value. The best value of the distance is that for which this second sum is minimized. Both of these sums are evaluated only over a certain range in phase within which our assumptions are valid. Ideally that is the whole cycle but as described subsequently the interval actually used was substantially less. Once this first pass is completed to derive final value of distance we should then iterate to correct our assumed surface gravity- ϕ relationship, but the problems described in § IVa were so much more serious that this was in fact never done.

b) Application to the Present Data

When this method is applied to our data, several practical problems manifest their existence. The photometric data set contains only about 90 pairs of points. Figure 2 illustrates the light curves B or i as a function of ϕ and we notice that there are several discrepant points in each light curve, most of which are from the last two rather cloudy nights. These points were smoothed onto the mean magnitude-color relationship. (This was done individually for each color, so that it is not necessarily true that the same points were smoothed in each color. The number of points thus treated ranged between two and

seven. Typical corrections in magnitude were ~ 0.05 mag for B or i .) Furthermore there are also up to four observations from the two cloudy nights with no B magnitudes, only i measurements. If for a particular star these fell into a phase interval where there were few points, they were added in with a smoothed B magnitude; otherwise they were ignored.

IV. RESULTS

a) Distances and Radii

The procedures described in § III have been applied to the data we obtained for the RR Lyraes in M5. Figure 3 shows the angular diameter-phase relationships used to determine the distance and mean radius for each of the variables. The crosses are from the individual B , i magnitude pairs and their locations are independent of the assumed distances and mean radii for the RR Lyrae variables. The solid curve is from the integration of the radial velocities using the distance which gives the best fit and the appropriate value of R_D . The filled squares represent the θ - ϕ relationship for the smallest distance which gave an acceptable fit, and the filled circles represent that for the largest possible distance which gave acceptable results. Figure 3a includes only those phases where T_{eff} is not more than 1000 K above the minimum value of T_{eff} . This removes an interval averaging 0.30 cycles centered on maximum visual light (minimum radius, maximum T_{eff} , maximum nongravitational acceleration). The resulting values of distance, mean radius, intensity mean absolute V magnitude, and distance modulus (the last two quantities both corrected for absorption) are listed in Table 4 for the best fit, as well as for the largest and smallest distances which yielded acceptable fits. These fits are in fact determined over a still smaller interval in phase as discussed later in this section. We also list the full amplitude of the radius variations over the period derived from integrating the radial velocity curve, which is independent of choice of distance but depends on the choice of projection factor p . The mean of the absorption corrected intensity mean V magnitudes for the four RR Lyrae stars in M5 is $+1.05$ mag, with a range of $+0.15$, -0.25 mag derived from averaging the limits of the acceptable fits given in Table 4. This is 0.25 mag fainter than

TABLE 4
DISTANCES AND MEAN RADII FOR M5 RR LYRAE STARS

Star	Distance (kpc)	Mean Radius (km)	Intensity Mean V_0	$(m - M)_0$	ΔR (km)
A. Best Fit					
M5-8	5.83	3.07E6	+1.21	13.83	533,600
M5-12	5.83	2.79E6	+1.20	13.83	504,000
M5-32	6.48	3.07E6	+0.95	14.06	501,700
M5-59	6.16	3.66E6	+0.93	13.95	470,300
B. Smallest Acceptable Distance					
M5-8	5.51	2.89E6	+1.33	13.71	
M5-12	5.51	2.63E6	+1.32	13.71	
M5-32	5.83	2.74E6	+1.18	13.83	
M5-59	5.51	3.29E6	+1.17	13.71	
C. Largest Acceptable Distance					
M5-8	6.48	3.41E6	+0.98	14.06	
M5-12	6.48	3.11E6	+0.97	14.06	
M5-32	7.12	3.36E6	+0.75	14.26	
M5-59	6.80	4.07E6	+0.72	14.16	

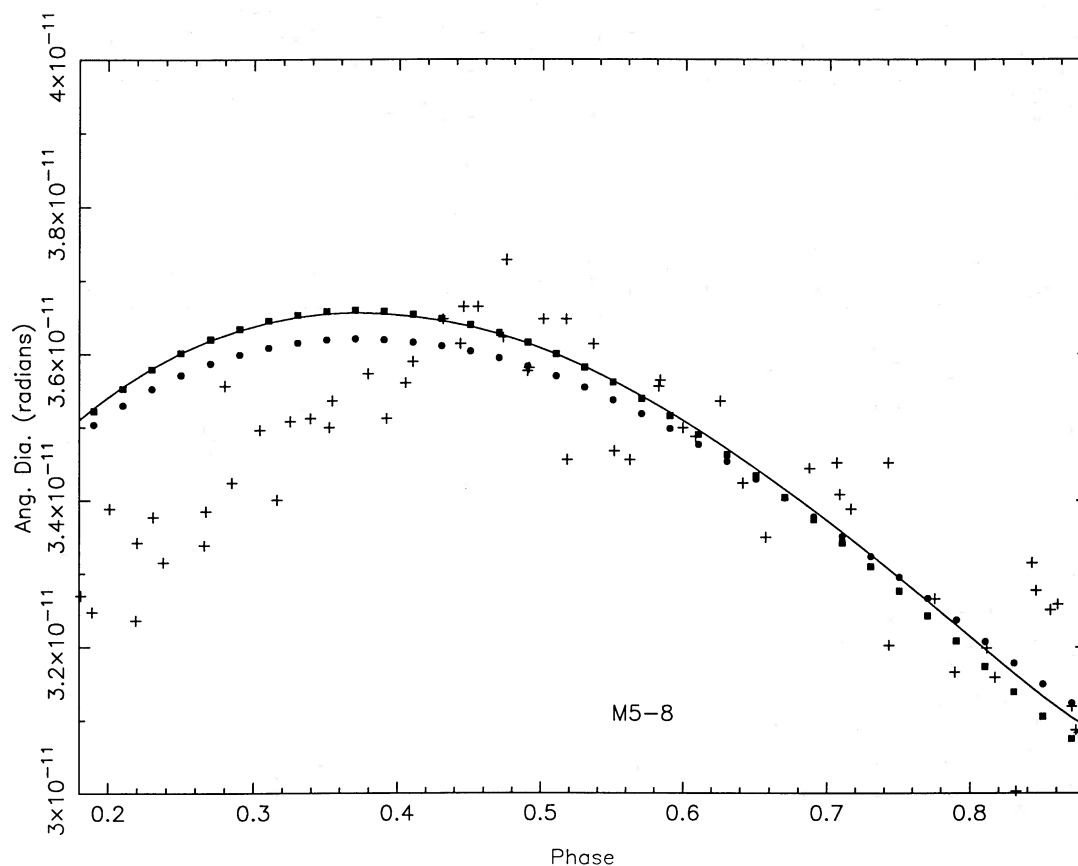


FIG. 3a

FIG. 3.—The angular diameter deduced from the photometric and from the spectroscopic data sets is plotted as a function of phase for the RR Lyrae star M5-8. The crosses represent the values of θ derived from each pair of B and i measurements. The solid curve is from the integration of the radial velocity curve with the choice of distance and the appropriate mean radius which gave the best fit between the two θ - ϕ relationships. The filled squares represent the θ - ϕ relationship for the smallest distance judged acceptable for this variable, while the filled circles illustrate the θ - ϕ relationship for the largest distance judged acceptable for this star. (b) Same as (a) for M5-12. (c) Same as (a) for M5-32. (d) Same as (a) for M5-59.

was adopted by Sandage (1982) for M5, resulting in a distance which is 89% as large as that of Sandage.

In spite of our effort at smoothing the photometry, the errors in our limited set of B and i magnitudes produce a significant scatter in the resulting $\theta(\phi)$ relationship. This directly produces the rather wide range of fits (hence of distances) which were judged acceptable. The scatter arises in part because for each star there are intervals in phase which contain a number of points which is too small to allow us to judge whether or not there are poor measurements included therein and how to properly smooth them. Thus in some cases the formal fitting procedure given above for determining the best distance fails due to the nonrandom distribution of photometrically determined $\theta(\phi)$ values about the $\theta(\phi)$ curve deduced from the radial velocities.

The major problem apparent from Figure 3 is the asymmetry of the photometric $\theta(\phi)$ curve compared to that from the radial velocities, which manifests itself as systematic deviation which increases progressively as one approaches maximum light ($\phi = 0$). This cannot be a phase shift in the data or a period error, as it has approximately the same sign and magnitude in all four variables, and the photometry and radial velocity data were obtained within a relatively short time interval for three of the four stars. This apparent asymmetry problem is seen in similar studies of field RR Lyrae variables (see Carney

and Latham 1984; Jones *et al.* 1987a, b). It is believed to be due to the effects of shocks lingering beyond the interval in phase around maximum light which we already omitted. If that is the case, at $\phi \approx 0.20$, overestimates of T_{eff} by about 250 K from our $B-i$ colors are required to bring the two $\theta(\phi)$ relationships into coincidence. This corresponds to an excessively blue $B-i$ color by about 0.13 mag, presumably arising largely from an excess flux in the blue spectral region due to perturbation of the atmosphere by shocks. The apparent overestimate of T_{eff} decreases progressively toward larger phases. Therefore in our distance determinations, the interval in phase used in the fitting was further restricted to 0.43 to 0.88 cycles for M5-8, 0.48 to 0.88 cycles for M5-12, 0.46 to 0.92 cycles for M5-32, and 0.45 to 0.88 cycles for M5-59. The fits determined over these intervals are those listed in Table 4 and plotted in Figure 3.

At this point, we recall that the range of distances listed for each star in Table 4 includes only the uncertainties arising from the limited available photometry and the small range in phase judged useful for matching the θ - ϕ curves. Although we cannot assess the systematic error that might result from the effects of the apparent phasing problem in fact lingering toward even later phases than the larger interval we have already discarded, we note that any such systematic error is likely to underestimate the angular diameter from the B, i photometry and hence overestimate the distance. Since our

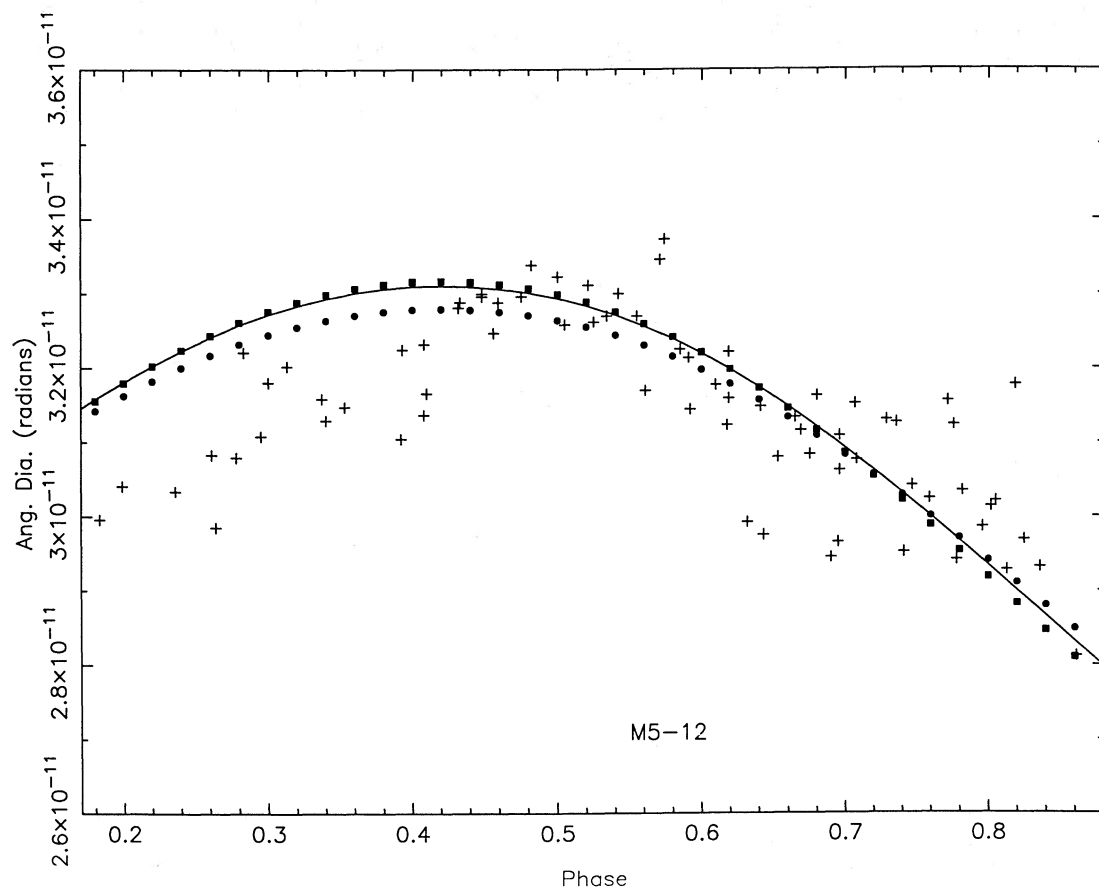


FIG. 3b

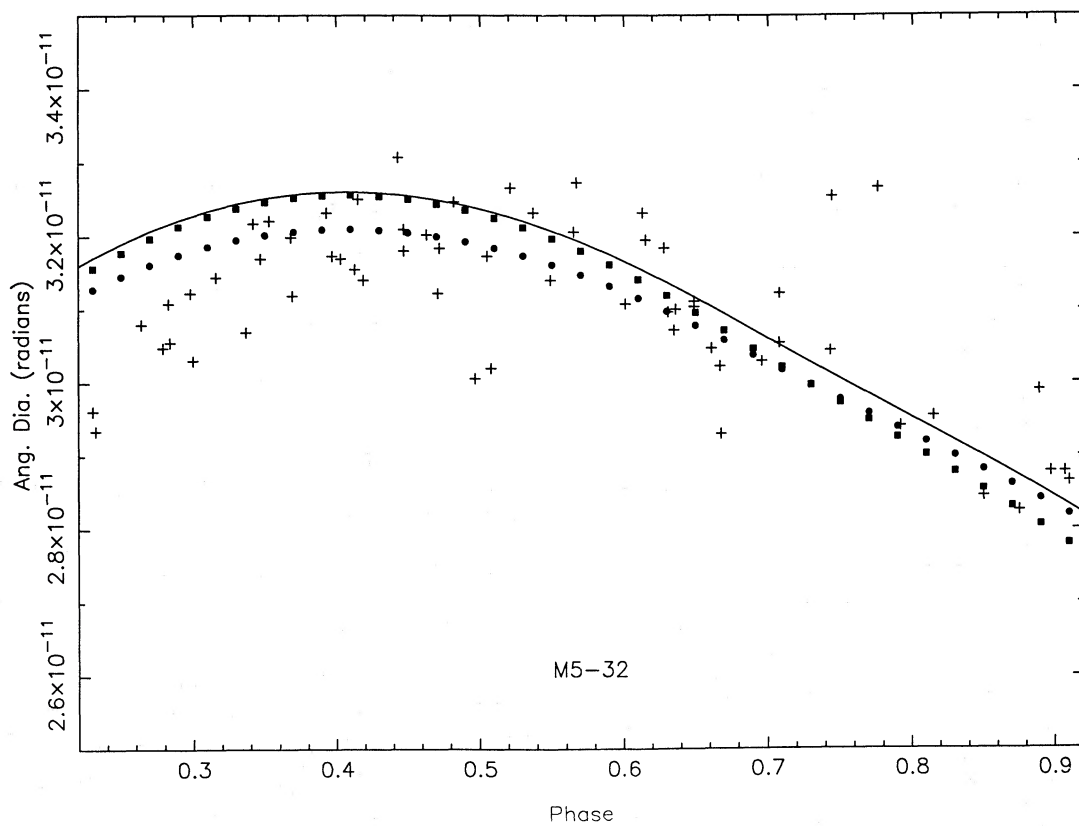


FIG. 3c

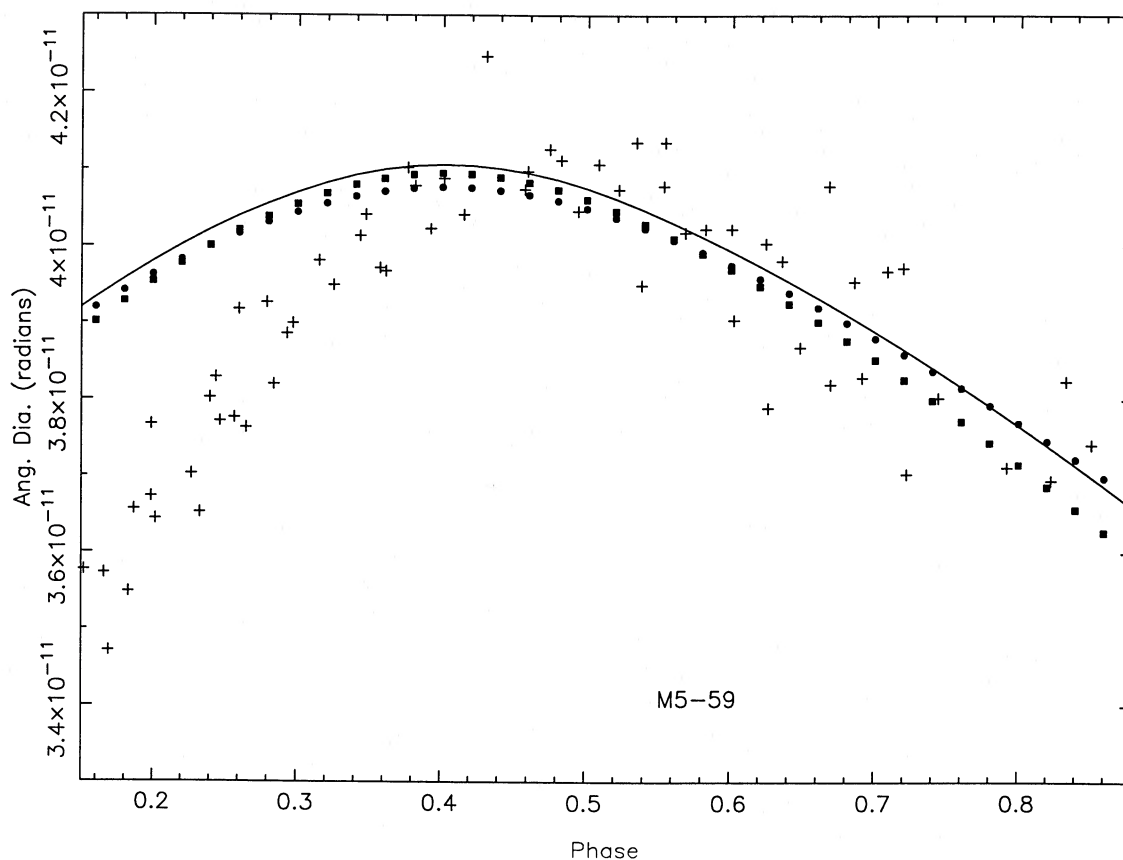


FIG. 3d

distance to M5 is already quite small, we feel that we have eliminated a sufficiently large interval in phase to remove any error arising from the apparent asymmetry, although this remains to be verified by further work planned for the 1986 observing season.

We now justify our assertion that several simplifications and assumptions which we glossed over earlier do in fact contribute only negligible errors to our distances. The uncertainty in the absolute calibration quoted by Oke and Gunn (1983) is 5% in the flux. The error made by neglecting the difference between 8100 Å and 8050 Å in evaluating the absolute flux is less than 0.005 mag, based on the tables of Oke and Gunn. The error made by ignoring the difference between the metallicity of M5 at about -1.5 dex and the models used (at -1.0 dex with respect to the Sun) is less than 4% in the absolute flux at 8050 Å. For a fixed $B-i$ color, the change in T_{eff} when the metallicity is changed from 0.1 to 0.01 that of the Sun is less than 100 K, which in turn corresponds to an error in the absolute flux at 8050 Å of less than 5%. Since the flux is proportional to D^{-2} , it is clear that the uncertainty in the distance we derive for the M5 RR Lyraes is dominated by the small regime in phase deemed acceptable and by the limited photometry within that regime of phase and the uncertainties in the photometry itself. Once the problems in the photometry are resolved, the small effects described above must of course be taken into account.

b) Comparison with Previous Applications of Baade-Wesselink Techniques to RR Lyrae Stars

The many previous studies of field RR Lyraes were listed in § 1. Without the extensive work of Carney and Latham (1984) and Jones *et al.* (1987a, b), we would be quite stumped by the apparent asymmetries in the light curves. Their work has demonstrated that these asymmetries become less significant when colors at redder wavelengths are used. In addition, they have shown that blue colors give results consistent with redder colors over only the latter part of the cycle, and we have used their results to guide us in choosing to reject the part of the cycle closest to maximum light when we fit for distance and mean radius. They too obtain magnitudes for the three RR Lyrae field stars which they have analyzed that are rather faint, averaging about $+0.85$ for magnitude-averaged, absorption-corrected absolute V magnitudes. Our only criticism of the analysis of Carney and collaborators is that since they do not use an automatic fitting program, but merely adjust radii and distances until a visually satisfying fit is obtained, it may be that their estimates of the uncertainty of their distances and absolute mean magnitudes due just to the fitting procedure are actually too small.

It is rather more difficult to compare our results to those of the CORAVEL group (Burki and Meylan 1986a, b and refer-

ences therein), who in general obtain brighter absolute mean magnitudes for the two field RR Lyrae stars for which they have published an analysis. This is because the most critical step in any Baade-Wesselink method is the determination of T_{eff} as a function of phase. Although they have multicolor photometry in the Geneva system, most of their colors are in the blue spectral region, and they have not published the details of their transformation between color and T_{eff} . They have noted the presence of excess ultraviolet light near maximum light in their analysis of RR Cet. The British group, whose progress is reviewed in Jameson (1986), used visual and infrared photometry on four field RR Lyrae stars to derive a strong metallicity dependence in the absolute mean V magnitudes, which was not found by Carney and his collaborators in a smaller sample of stars. Their temperature determinations are derived by assuming a linear relationship between color and $\log(T_{\text{eff}})$ whose coefficients are empirically determined from the observations of the RR Lyrae variable itself. This is a variation of the method of Balona (1977). A detailed critique of the approaches used by both of these groups can be found in Jones *et al.* (1987b).

It is clear that no such result from an application of the Baade-Wesselink method to RR Lyrae stars can be fully trusted until the extent of the flux discrepancy is mapped as a function of phase and wavelength. The critical assumption that a series of static model atmospheres may be applied to successive phases of a pulsating variable star with a short period is made in some form by all groups working in the field. This gives rise to the major uncertainty affecting RR Lyrae distances today. Hopefully we will obtain the necessary data during the coming year to satisfy ourselves that within some limits of phase and wavelength Baade-Wesselink techniques can in fact be used to determine accurate distances for RR Lyrae variables.

V. SUMMARY

The observational material necessary for the application of the Baade-Wesselink method of determining distances has been obtained for four RR Lyrae variables in the globular cluster M5. We have measured radial velocity-phase curves from spectra taken with the 200 inch Hale telescope at Palomar Observatory. We have between 28 and 56 independent values per star with an accuracy no worse than $\pm 4 \text{ km s}^{-1}$ per radial velocity. Light curves for the four RR Lyrae stars have been obtained using an imaging CCD system at the 60 inch telescope at Palomar Mountain. We took short exposure frames through a Johnson B and a near-infrared i filter. The photometric and the spectroscopic data sets were obtained within a 6 week interval in 1986 April–May, except for the RR Lyrae star M5-32, which was also observed spectroscopically in 1985. About 90 pairs of B and i magnitudes are available for each star. There are also light curves for six additional RR Lyrae variables in M5 that fell within the area covered by the two CCD fields. These light curves have been transformed to V magnitudes, then integrated to yield mean and intensity mean V magnitudes for each variable.

The method of analysis which has been developed for the data requires matching the angular diameter-phase relationship determined from the spectroscopic and from the photo-

metric data sets. The treatment of the spectroscopic data is straightforward. The v_r - ϕ relationship is integrated using a projection factor to convert between radial velocity and pulsational velocity of 1.31. The mean velocity (v_r) of each of the four RR Lyrae stars is within 4 km s^{-1} of the measured radial velocity of M5 itself as compiled by Webbink (1981). If one assumes a value for the distance to M5 and a value of the stellar radius at $\phi = 0$, the spectroscopic θ - ϕ relationship is easily obtained. The photometric data is treated by using an effective wavelength for the B and the i filters, assuming that the absolute calibration of observed flux from the bright spectrophotometric standards by Oke and Gunn (1983) is correct, and transforming the observed magnitude at i into a flux above Earth's atmosphere. This is compared with an emitted flux per unit of radiating area from the appropriate model stellar atmospheres of the grid by Kurucz (1979) at the effective wavelength of the i filter. The effective temperature is deduced from the B , i colors (with the metallicity and gravity dependence taken into account as discussed in detail in § IIIa).

The distance and mean radius are derived by fitting algorithms which match the spectroscopically and photometrically derived θ - ϕ curves. Averaging the results from the four M5 RR Lyraes analyzed in detail, this procedure yields an intensity mean, interstellar absorption-corrected V magnitude of $+1.05 \text{ mag}$. Because of the limited photometry, its limited accuracy (two of the nights used were cloudy, and sometimes data from these nights fell in critical regions of phase), and the limited region of phase that could be used to deduce the distance, the fitting errors alone permit values up to $+0.15 \text{ mag}$ fainter or -0.25 mag brighter. This does not include any systematic errors or uncertainties arising from the method of analysis, which are believed to be small compared to the fitting uncertainties, or from the limited region in phase that was used due to asymmetry problems in the light curves. These asymmetry problems which have been seen in other investigations of field RR Lyrae variables utilizing blue colors (see, for example, Carney and Latham 1983), greatly restrict the range of phase that can be used to derive the distances, eliminating a substantial interval in phase beginning just before maximum visual light.

After a review of existing field star Baade-Wesselink analyses, we find that the primary remaining area of concern is the applicability of a set of static stellar atmospheres to a pulsating variable star at a given phase. We plan to test the validity of this procedure to determine the limits of phase and wavelength over which such an approach is accurate. Although we believe that by eliminating a substantial interval in phase and by determining the flux at a near-infrared color we have avoided the worst of these problems, it is nonetheless true that until these limits have been determined, all distances derived from Baade-Wesselink analyses of RR Lyrae stars must be regarded with some degree of skepticism.

This work was initiated under NSF grant AST-8212270. J. G. C. is grateful to the Caltech Recycling Center and to Gaston Araya Machining for financial and other support. G. A. G. was supported during part of the time by a Caltech Summer Undergraduate Research Fellowship.

REFERENCES

- Abt, H. A., and Biggs, E. S. 1972, *Bibliography of Stellar Radial Velocities* (New York: Latham Process Co.).
- Arp, H. C. 1962, *Ap. J.*, **135**, 311.
- Baade, W. 1926, *Astr. Nach.*, **228**, 359.
- Bailey, S. I. 1917, *Harvard Ann.*, **78**, 103.
- Balona, L. A. 1977, *M.N.R.A.S.*, **178**, 231.
- Barnes, T. G., III, and Hawley, S. L. 1986, *Ap. J. (Letters)*, **307**, L9.
- Bell, R. A., and Oke, J. B. 1986, *Ap. J.*, **307**, 253.
- Burki, G., and Meylan, G. 1986a, *Astr. Ap.*, **156**, 131.
- . 1986b, *Astr. Ap.*, **159**, 255.
- Cacciari, C. 1986, private communication.
- Carney, B. W. 1980, *Ap. J. Suppl.*, **42**, 481.
- Carney, B. W., and Latham, D. W. 1984, *Ap. J.*, **278**, 241.
- Coutts, C., and Sawyer-Hogg, H. 1969, *Pub. David Dunlop Obs.*, Vol. 3, No. 1.
- Dreiling, L. A., and Bell, R. A. 1980, *Ap. J.*, **241**, 736.
- Frogel, J. A., Cohen, J. G., and Persson, S. E. 1983, *Ap. J.*, **275**, 773.
- Graham, J. A. 1984, in *IAU Symposium 108, Structure and Evolution of the Magellanic Clouds*, ed. S. van den Bergh and K. S. de Boer (Dordrecht: Reidel), p. 207.
- Graham, J. A., and Nemec, J. M. 1984, in *IAU Symposium 108, Structure and Evolution of the Magellanic Clouds*, ed. S. van den Bergh and K. S. de Boer (Dordrecht: Reidel), p. 37.
- Gunn, J. E., and Griffin, R. 1979, *A.J.*, **84**, 752.
- Hanbury Brown, R., Davis, J., and Allen, L. R. 1974, *M.N.R.A.S.*, **167**, 121.
- Hawley, S. L., Jeffreys, W. H., Barnes, T. G., III, and Lai, Wan. 1986, *Ap. J.*, **302**, 626.
- Hindsley, R. and Bell, R. A. 1986, *Pub. A.S.P.*, **98**, 881.
- Hogg, H. S. 1973, *Pub. David Dunlop Obs.*, Vol. 3, No. 6.
- Jameson, R. F. 1986, *Vistas Astr.*, **29**, 17.
- Jones, R. V., Carney, B. W., Latham, D. W., and Kurucz, R. L. 1987a, *Ap. J.*, **312**, 254.
- . 1987b, preprint.
- Kurucz, R. L. 1979, *Ap. J. Suppl.*, **40**, 1.
- Longmore, A. J., Fernley, J. A., Jameson, R. F., Sherrington, M. R., and Frank, J. 1985, *M.N.R.A.S.*, **216**, 873.
- Manduca, A., and Bell, R. A. 1981, *Ap. J.*, **250**, 306.
- Manduca, A., Bell, R. A., Barnes, T. G., III, Moffett, T. J., and Evans, D. S. 1981, *Ap. J.*, **250**, 312.
- Oke, J. B. 1966, *Ap. J.*, **145**, 468.
- Oke, J. B., and Gunn, J. E. 1983, *Ap. J.*, **266**, 713.
- Oort, J. H., and Plaut, L. 1975, *Astr. Ap.*, **41**, 71.
- Pritchett, C. J., and van den Bergh, S. 1986, preprint.
- Sandage, A. 1970, *Ap. J.*, **162**, 841.
- . 1982, *Ap. J.*, **252**, 561.
- Schneider, D. P., Gunn, J. E., and Hoessel, J. G. 1983, *Ap. J.*, **264**, 337.
- Strugnell, P., Reid, N., and Murray, C. 1986, *M.N.R.A.S.*, **220**, 413.
- Thuan, T. X., and Gunn, J. E. 1976, *Pub. A.S.P.*, **88**, 543.
- Wade, R. A., Hoessel, J. G., Elias, J. H., and Huchra, J. P. 1979, *Pub. A.S.P.*, **91**, 35.
- Webbink, R. F. 1981, *Ap. J. Suppl.*, **45**, 259.
- Wesselink, A. J. 1969, *M.N.R.A.S.*, **144**, 297.
- Zinn, R. J. 1980, *Ap. J. Suppl.*, **42**, 19.

J. G. COHEN and G. A. GORDON: 105-24, California Institute of Technology, Pasadena, CA 91125